Core Poloidal Rotation and Internal Transport Barrier Formation in TFTR

R E Bell[†], F M Levinton[‡], S H Batha[‡§], E J Synakowski[†], M C Zarnstorff[†]

[†]Princeton Plasma Physics Laboratory, Princeton, New Jersey 08543

[‡]Fusion Physics and Technology, Torrance, California 90503

Abstract. Impurity poloidal rotation velocities have been measured in the core of TFTR plasmas using a new spectroscopic diagnostic. Two types of transitions to enhanced confinement in reversed shear plasmas are examined. A bifurcation in carbon poloidal rotation is observed to occur before the transition to enhanced confinement for one of these types, while other measured plasmas parameters remain constant. A narrow radial region with reversed poloidal rotation and rotational shear is established 60-100 ms before the transition, and is associated with a large negative radial electric field.

1. Introduction

Tokamak plasmas with negative central magnetic shear have exhibited desirable confinement characteristics within a core transport barrier (Levinton *et al* 1995, Strait *et al* 1995). A complete understanding of the dynamics of barrier formation requires accurate measurements of all quantities in the radial force balance equation,

$$E_r = \nabla p \, / \, (eZn) + v_\phi B_\theta - v_\theta B_\phi \, ,$$

where p is the ion pressure, e is the electronic charge, Z is the charge number, n is the ion density, v_ϕ and v_θ are the toroidal and poloidal velocity, B_ϕ and B_θ are the toroidal and poloidal magnetic fields. The carbon pressure and toroidal velocity have routinely been measured on TFTR using charge exchange recombination spectroscopy. Presented here are

---

[§] Present address: Science Research Laboratory 15 Ward St. Somerville, MA 02144

new measurements of carbon v_θ profiles and E_r in the core of TFTR plasmas and their connection to the formation of transport barriers in enhanced reversed shear (ERS) plasmas.

In TFTR ERS plasmas, two types of transitions to improved confinement have been observed (Bell *et al* 1996). Though they share improvements in particle, ion thermal and momentum confinement, they differ significantly in power threshold ($\approx$ 20 MW for Type I, $\leq$ 5 MW for Type II). Type I transitions show a sudden increase $\partial n_e/\partial t$ within the core, while Type II transitions are marked by an abrupt increase in T_i and T_e. Type I transitions, using neoclassically calculated values of v_θ, are consistent with $E \times B$ shear flow suppression of turbulence as a triggering mechanism (Bell *et al* 1996, Synakowski *et al* 1997). Type II transitions were found to occur with a variety of E_r profiles, suggesting no clear link to $E \times B$ shear flow as a trigger mechanism. Despite the low power threshold, Type II transitions were only observed late in the discharge at similar times when $q_{min} \gtrsim 2$, suggesting a link with the evolving current density profile.

2 Experimental

The v_θ measurements were made using a new spectroscopic diagnostic designed to measure carbon poloidal velocities in the core of TFTR plasmas using the Doppler shift of the C VI 5291 Å impurity line. The diagnostic had a 20 ms time resolution and a radial resolution of $\leq$ 3.5 cm after an inversion (Bell 1997) is applied. All v_θ data shown here are chord-averaged. The motional Stark effect (MSE) diagnostic (Levinton *et al* 1989), which measures the pitch angle of the magnetic field lines, is also sensitive to E_r (Zarnstorff *et al* 1997).

During the startup of Type I ERS plasmas, a current ramp was used with early low power neutral beam injection to produce a hollow current profile. Higher neutral beam power was then added in a heating phase. Lithium pellet injection, which has proven to be useful in achieving conditions favorable for a transition, was used during the early low power phase. Typical parameters were R_0 = 260 cm, and B_T = 4.6, 3.4 T. The higher field is typical for most TFTR ERS discharges. The neutral beam power during the heating phase, P_{NB}, was typically 25-28 MW for high B_T discharges, and 13-15 MW for low B_T discharges. The plasma current $I_{\rm p}$=1.6 /1.2 MA was used in the high/low field discharges, which were set up to have nominally the same edge q.

The startup of ERS plasma with a Type II transitions was similar with $B_{\rm T}$=4.8 T, I_p = 1.6 MA, P_{NB} = 13 MW. The Li pellet was injected at the start of the heating phase.

3. Results

Two reversed shear discharges are seen to undergo a bifurcation in confinement shortly after the start of the high power heating phase, as indicated by the carbon pressure in Fig. 1a. Shown in Fig. 1b is the chord-averaged carbon v_θ for these two discharges, which diverged before the transition. The carbon ions at this location which had been rotating in the positive (ion diamagnetic) direction began a reversal in direction about 60 ms before the first indication of a confinement improvement. The excursion in rotation peaks and then relaxed as the confinement improvement took place. This change in v_θ was radially localized, typically appearing on only one or two viewing chords.

Much larger changes in the v_θ precursor are sometimes seen in the lower field experiments ($B_{\rm T}$=3.4 T). Figures 2 and 3 show the chord-averaged v_θ in a narrow radial region change by more than 40 km/s prior to the ERS transition. The full magnitude of the negative velocity is reduced by the chord averaging of the data. This large negative v_θ corresponds to a large negative E_r . Shown in Fig. 2b is the change in E_r as determined by the MSE diagnostic; the change is E_r is so large, localized, and rapid that its contribution to the measured polarization angle is readily separable from the slowly changing magnetic field contribution. There is a strong temporal and spatial correlation between the measured v_θ and the measured change in E_r .

Two poloidal velocity profiles are plotted against the tangency radii of the sightlines in Fig. 3. The large negative well that develops in the poloidal velocity profile is narrower than it appears. Sightlines interior to the shear layer include diminishing samples of the negative velocity region. The radial extent of this high velocity shear region was small compared to the spatial separation of the v_θ sightlines (3.5 cm) or the MSE sightlines (4 cm). Comparison of the v_θ profile and the measured q profile in Fig. 3 indicates that the location of the negative velocity region was a few centimeters *inside* of the radial location of the minimum in the safety factor, q_{min}.

Poloidal rotation measurements for a Type II ERS transition are shown in Fig. 4. The central ion temperature $T_i(0)$ increased suddenly by 60% at the transition. There was a smaller increase in T_e, with little change in n_e or v_ϕ. The electrons are presumably being heated by the ions, since, like the Type I ERS plasmas, there is no apparent improvement in the electron thermal conductivity after the transition. No change in v_θ was seen before the transition. After the transition, v_θ increased, consistent with the increase in ∇p due to the increased T_i. Using the inversion point of the normalized heating rate ($1/T_e\ dT_e/dt$) from ECE measurements, for similar Type II discharges, the location of the transport barrier was found to be a few centimeters *outside* of the location of q_{min}. (see Fig. 4 in Bell *et al* 1996)

4. Discussion

The proposed role of $E \times B$ shear in the formation of the transport barrier is reinforced for the Type I ERS transition by the new core poloidal velocity measurements.

At least for one discharge, though, no poloidal velocity precursor was observed before the ERS transition, indicating perhaps that the observed poloidal excursion is not a necessary condition for a transition. There is no clear generating mechanism for the poloidal excursion and negative E_r at this time. There are remarkable similarities between the linked behavior of v_θ and E_r in the core to those observed at L-H transitions at the edge. Some of the proposed mechanisms for the generation of the E_r at the edge warrant investigating in the core.

The neoclassical calculations of the poloidal velocity, previously used on TFTR to evaluate the role $E \times B$ shear played in the formation and sustainment of the transport barrier, of course, could not anticipate the dynamics of the large poloidal velocity and the velocity shear observed. Differences between measured and neoclassically calculated v_θ may explain the differences in the calculated turbulence growth rate and the shearing rate at the time of transition for low field discharges (Levinton *et al* 1996). This will be addressed in future work.

The differences in the power threshold, the timing, the poloidal rotation, and the location of the barrier at transition suggest the Type II transition has a different triggering mechanism than the Type I transition.

Acknowledgement

This work has been supported by the US Department of Energy Contract No. DE-AC02-76-CH03073.

References

Bell R E *et al* 1996 *Proc. 23rd EPS Conference on Controlled Fusion and Plasma Physics (Kiev)* **20C** Part I p 59

Bell R E 1997 Rev. Sci. Instrum. **68** 1273

Levinton F M *et al* 1989 Phys. Rev. Lett. **63** 2060

Levinton F M *et al* 1995 Phys. Rev. Lett. **75** 4417

Levinton F M et al 1996 Proc. 16th International Conference on Fusion Energy (Montreal, 1996) (IAEA, Vienna, 1997) IAEA-CN-64/A1-3 Vol. 1 p 211

Strait E J *et al* 1995 Phys. Rev. Lett. **75** 4421

Synakowski E J *et al* 1997 Phys. Plasmas **4** 1737

Zarnstorff M C *et al* 1997 Phys. Plasmas **4** 1097

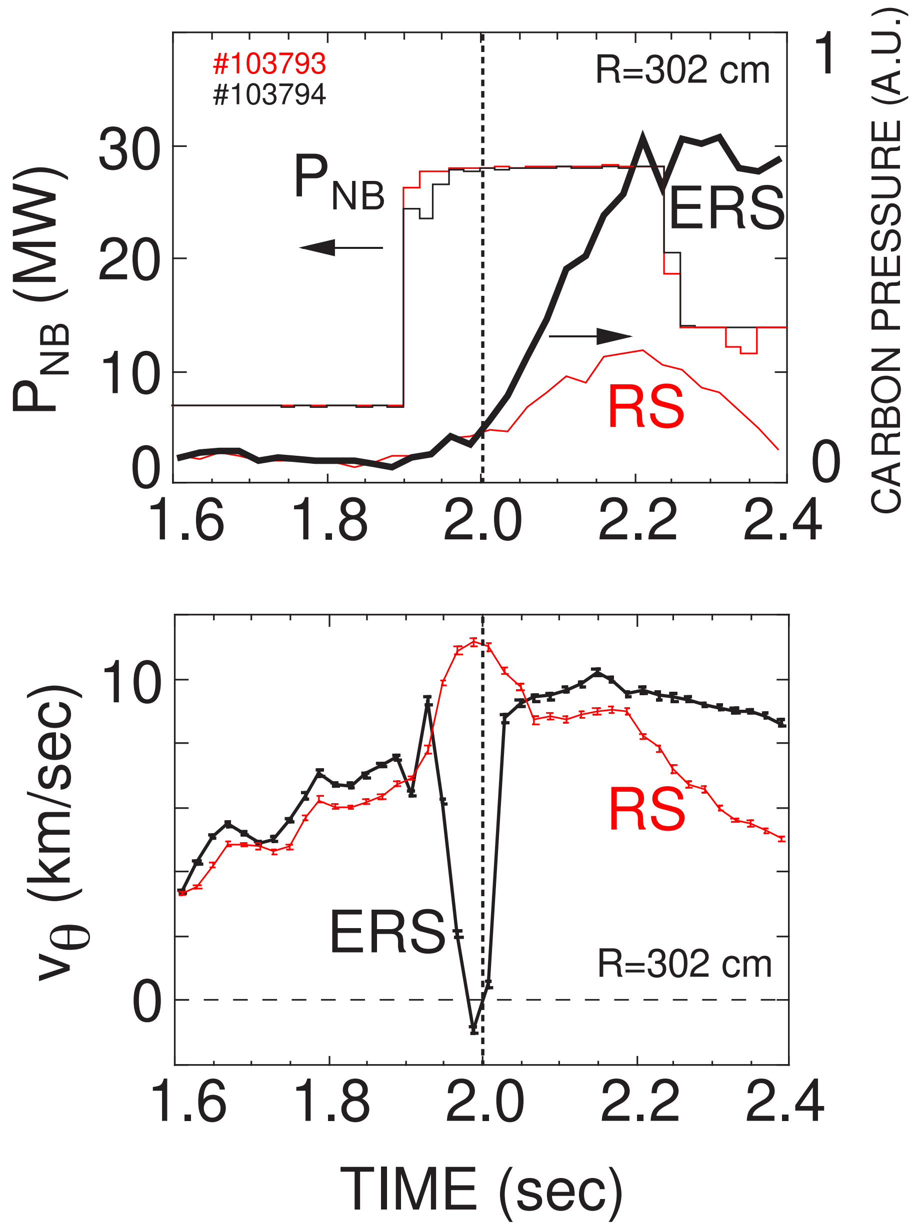

Fig. 1 Comparison of two reversed shear discharges. (a) The ERS transition time is indicated by the bifurcation in the local carbon pressure. (b) A bifurcation in the carbon poloidal velocity occurs before the transport improvement. Positive values of v_θ are in the ion diamagnetic drift direction.

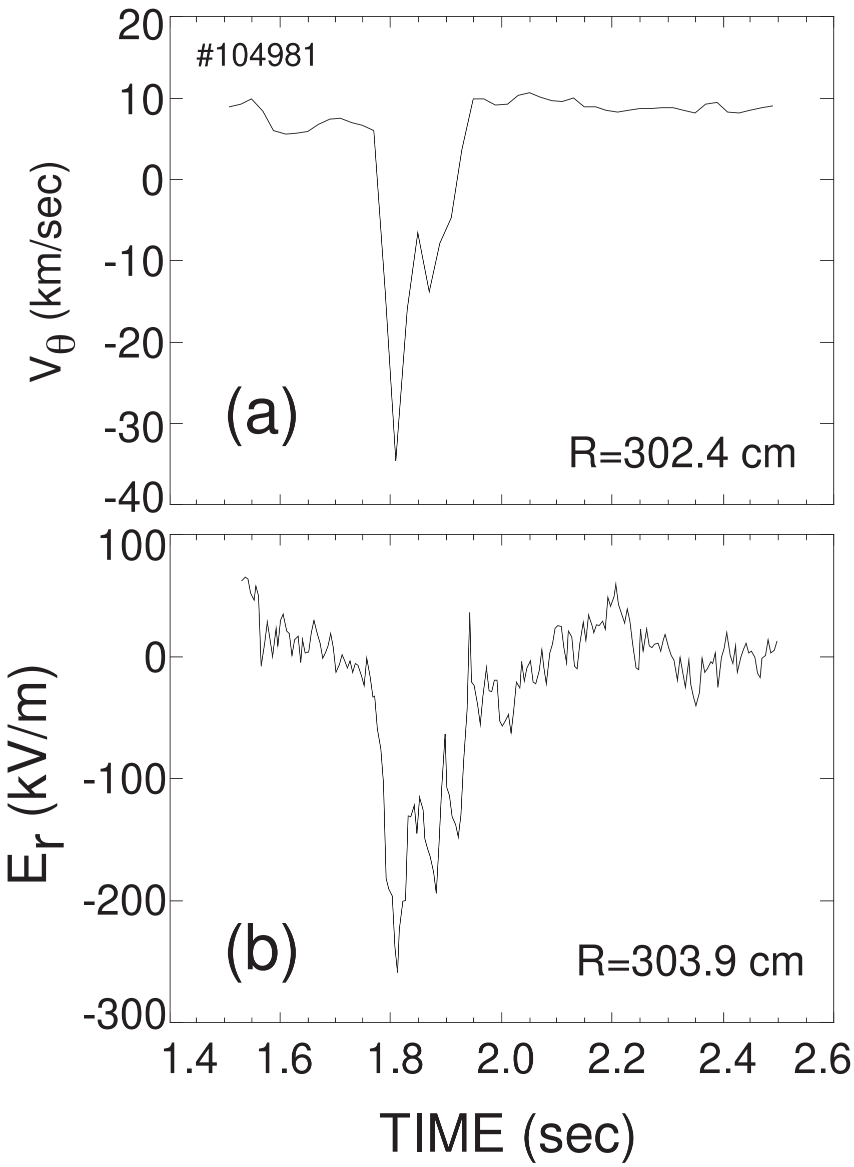

Fig. 2 Measured carbon v_θ and E_r show similar time behavior. (a) A large excursion in v_θ is observed in a low field (B_T = 3.4 T) ERS discharge on a single sightline (b) Change in E_r measured by MSE diagnostic

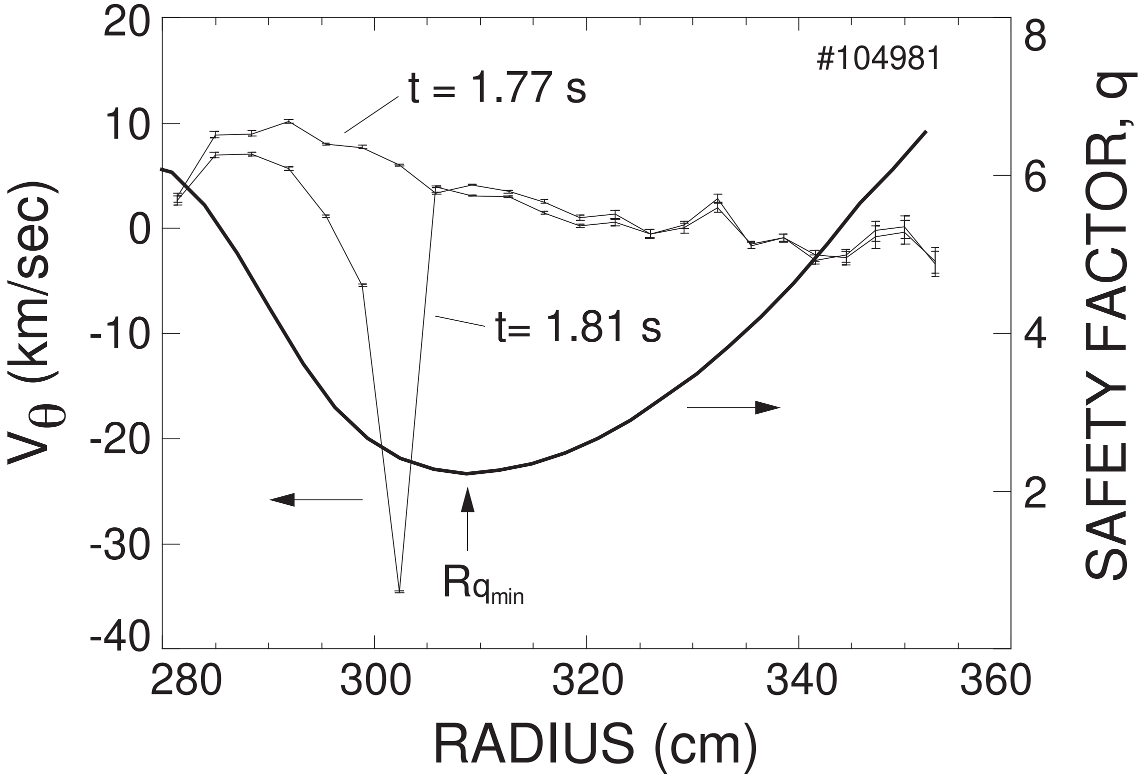

Fig. 3 Carbon poloidal rotation profiles at two times before the ERS transition, before and during the local excursion in v_θ . Overlaid is the measured q profile. The location of the velocity shear layer is just inside of the location of q_{min}.

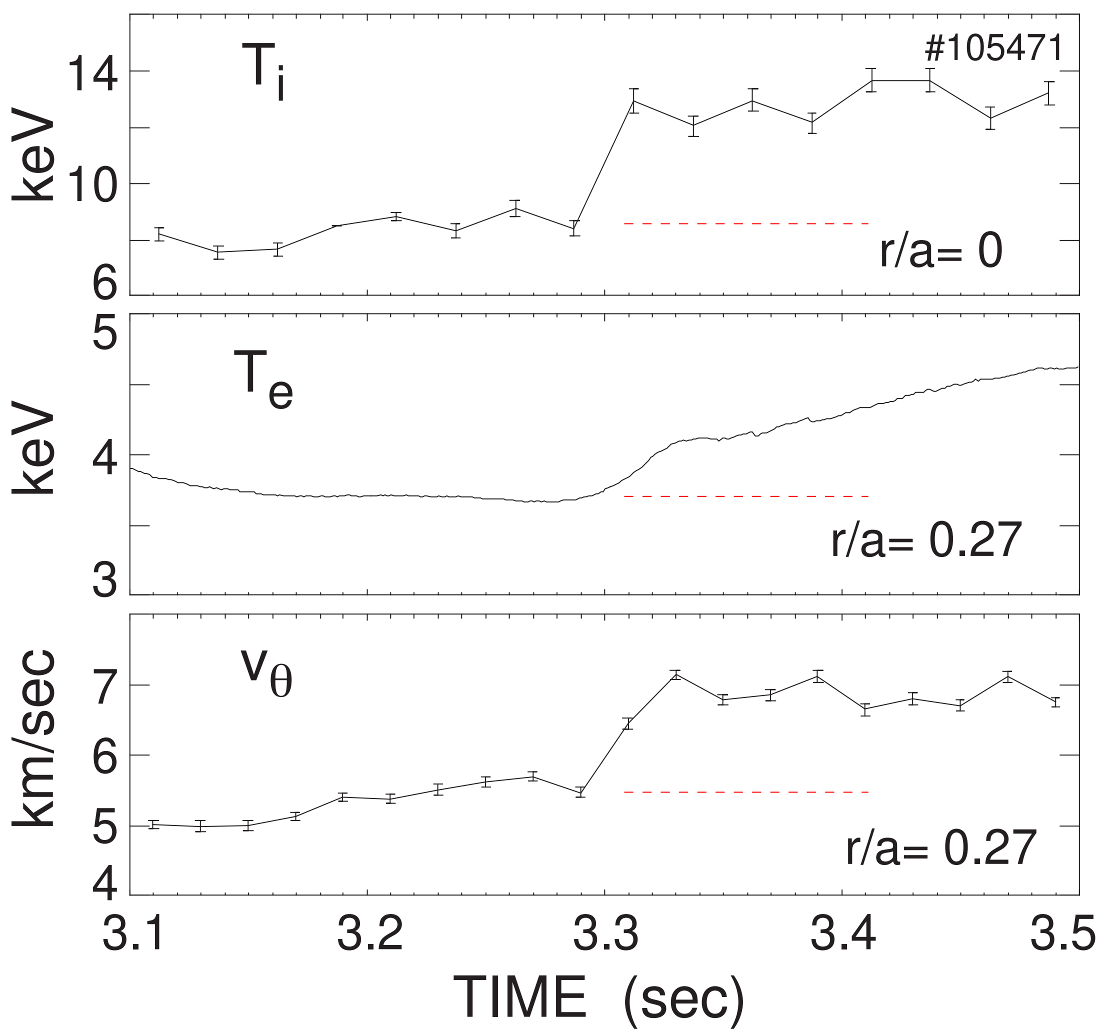

Fig. 4 The time behavior of T_i and T_e across the Type II ERS transition. No poloidal rotation change is observed before the transition.